Engineering Solutions to Mechanics, Marine Structures and Infrastructures

Eng. Solut. Mech. Mar. Struct. Infrastruct.
2024.1(4).1
ISSN：3006-2837
https://doi.org/10.58531/esmmsi/1/4/1

Article

Design of a Crab-like Underwater Robot Control System

Yutao Tian, Tiande Li, Ying Xue, Yihao Zhang, Dapeng Zhang*

Ship and Maritime College, Guangdong Ocean University, Zhanjiang 524005 China.

Academic Editor: Weiwei Wang <zhwangww@ytu.edu.cn>

Received: 29 September 2024; Revised: 20 October 2024; Accepted: 23 October 2024; Published: 24 October 2024

Abstract: To address issues encountered by underwater robots during operations, such as damage or reduced efficiency due to complex underwater terrains and strong water currents, a robot inspired by the adaptability of crabs to various terrains has been designed. This robot employs a crab-like structure equipped with anti-displacement legs and utilizes superconducting magnetic fluid propulsion and sacrificial anode inspection devices. This article mainly analyzes the parts mentioned of the robot, demonstrating that the robot can reduce underwater operation costs and improve underwater working efficiency. The design aims to assist in the mid to late stages of oil and gas development exploration and maintenance, providing new guidance and recommendations for the laying, inspection, and maintenance of oil and gas pipelines.

Keywords: Underwater robot; Sacrificial anode inspection; Bioinspired;

1. Introduction

The ocean resources on Earth are extremely rich, with large quantities of valuable mineral and oil and gas resources hidden in deep-water regions that humans cannot easily access, necessitating the use of underwater robots for exploration and extraction [1]. At the same time, underwater robots are also essential for the laying and maintenance of underwater cables and oil and gas pipelines, as well as the maintenance of marine platforms and other equipment. Underwater vehicles generally include Autonomous Underwater Vehicles (AUV), Remotely Operated Vehicles (ROV), Manned Submersibles, and Glider.

Citation: Tian Y., Li T., Xue Y., Zhang Y., Zhang D. Design of a Crab-like Underwater Robot Control System. Eng. Solut. Mech. Mar. Struct. Infrastruct., 2024, 1(4), doi: 10.58531/esmmsi/1/4/1

In China, underwater robots are a very popular topic. Research on bionic underwater robots involves comparing the remarkable structures and behavioral characteristics of organisms in nature and applying these aspects to the design of robots, simulating their underwater operations in real environments. In 2023, Junhao Zhang and others studied the modeling and control simulation of underwater serpentine robots [2]. In 2024, Xuehai Zhang and others designed a bionic squid underwater sampling manipulator [3], and the same year, Dongdong Zhang and colleagues designed an underwater robot based on the bionic jellyfish [4]. Table 1 provides an overview of the movement characteristics of the aforementioned robots and the crab-like underwater robot discussed in this article.

Table 1. Overview of the movement characteristics of different robots

Snake-like underwater robot	Uses undulating and flexible movement, exhibiting high maneuverability. It can adapt to complex environments and navigate through narrow spaces. Energy consumption is relatively high.
bionic squid underwater sampling manipulator	Simulates biological movement characteristics and has good grasping ability. However, the structural design is complex, making maintenance difficult
Jellyfish-like underwater robot	Moves freely in water with high degrees of freedom, exhibiting flexible motion and low energy consumption. It requires higher control precision.
Crab-like Underwater Robot Anti-displacement crab legs	High stability, suitable for rugged seabed environments. But the movement space of the limbs is limited, leading to slower movement speed.

Excluding the research conducted by Chinese scholars on underwater biomimetic robots, international scholars have also made significant contributions to the related topic of underwater biomimetic robots. In 2022, Souad Larabi-Marie-Sainte and others developed the metaheuristic algorithm LBIUSR-MA to study bio-inspired underwater snake robots [5]. In 2024, Eliseo de J. Cortés Torres and colleagues designed a bio-inspired device with three active degrees of freedom for the pectoral fins by simulating the coordinated movements of stingray fins [6]. Numerous new research projects indicate that the research and design of bio-inspired underwater robots have received significant attention.

This underwater robot specifically refers to the natural movement of crabs in biomimicry, combining mechanical engineering science and kinematics to design a crab-like underwater robot. Figure 1 and Figure 2 show the appearance and details of the robot. The crab dome-shaped head shell effectively reduces water flow resistance, while the anti-displacement crab legs and superconducting magnetic fluid propulsion system enable the robot to navigate the seabed with multiple degrees of freedom. The front claws and anti-displacement crab legs can easily cut through obstacles, enhancing the robot's ability to adapt

to various terrains. The bionic structure based on biological prototypes demonstrates good impact resistance and durability. The propulsion system uses a new type of superconducting magnetic fluid propulsion, which offers significant advantages over traditional propeller propulsion, including contactless propulsion, low energy consumption, reduced noise, and operational safety. The two mechanical arms at the front claws allow for the sampling of preliminary samples and maintenance of oil and gas pipelines. Six anti-displacement crab legs can secure the robot to any position on the seabed, enhancing its maneuverability. The robot's lower abdomen is equipped with a sacrificial anode detection device for maintaining and repairing underwater oil and gas pipelines, improving the robot's efficiency and extending its mechanical endurance. This type of bionic robot has a complete structure and full functionality, with promising prospects for engineering applications.

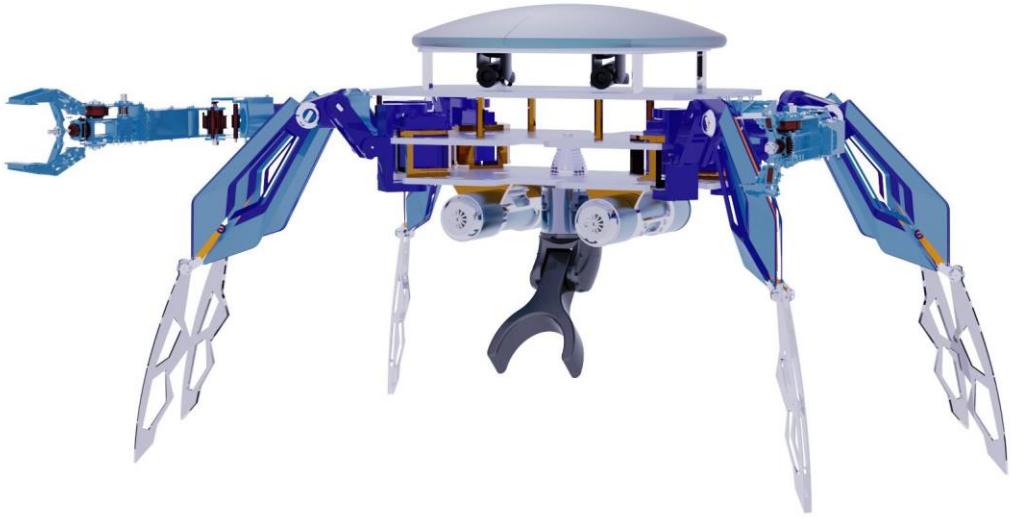

Figure. 1. Actural appearance of the robot.

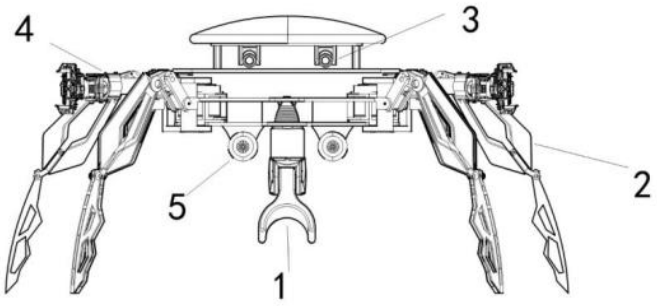

Figure. 2. Main structure of the robot. 1-Sacrificial anode inspection devices 2-Anti-displacement crab legs 3-Vision system 4-Mechanical arm 5-Superconducting magnetic fluid propulsion device.

2. Main structure of the robot

2.1 New-type superconducting magnetic fluid propulsion device

First, this Superconducting magnetic fluid propulsion device uses titanium-chromium alloy [7] for its shell. Titanium-chromium alloy has excellent hydrophobic properties [8],

which can effectively reduce the resistance encountered by the robot underwater. Additionally, titanium-chromium alloy has high hardness, preventing deformation of the underwater robot due to accidental impacts or excessive pressure differentials inside and outside the device, allowing the robot to operate in deeper underwater environments. Furthermore, a polyurethane coating is applied to the surface of the device; its excellent weather resistance [9] ensures that the metal surface remains protected from corrosion under varying water pressures at different depths.

Magnetic fluid propulsion is a way of propulsion that does not rely on traditional propellers. Compared to traditional propulsion devices like propellers and water jets, this device uses seawater as the conductive fluid and directly promotes the fluid through the interaction of electromagnetic fields, thereby generating thrust, reducing the noise generated by the large-scale mechanical vibration of the traditional propulsion method and the dangers of propeller cavitation [10]. The device uses superconductors as solenoids, generating a strong magnetic field when powered on, and the fluid cuts through the magnetic flux lines to achieve further propulsion. By integrating the gas-liquid two-phase flow technology with fluid dynamics driven by a superconducting magnetic field, the thrust is significantly enhanced and the energy efficiency is greatly improved. At the same time, the bubble mixing chamber and the bubble generator are added to the superconducting magnetic fluid propulsion device, achieving efficient mixing of the gas-liquid two-phase flow [11]. When the seawater flows through the propulsion device, it will be affected by the magnetic field generated by the superconducting magnet to generate thrust. When the seawater subjected to thrust enters the bubble mixing chamber, the high-pressure gas is injected into the chamber and transported to the bubble generator to disperse to form bubbles, and then mixed with the seawater in the bubble mixing chamber to form a bubble flow [12], and then, it accelerates to eject through the outlet pipe [13]. This method not only uses the magnetic field force generated by the superconducting magnet to directly push the seawater, but also further converts the gas pressure into the kinetic energy of the water flow through the expansion effect of the bubble. At the same time, if underwater robots can achieve superconductivity during linear propulsion, it greatly reduces energy consumption. Compared with the general propulsion device, this propulsion method significantly enhances its propulsion efficiency and thrust, and can reduce energy consumption.

As shown in Figure 3, the superconducting magnetic fluid propulsion device realizes the real-time feedback control of the propulsion system through the linkage of the built-in speed sensor and the speed control device, and the speed sensor obtains accurate speed measurement value to carry out the specific control of the robot speed. The device interacts with the system through different current signals, allowing for automatic adjustment of current intensity and magnetic field distribution as needed, optimizing propulsion efficiency while ensuring smooth navigation and fuel economy.

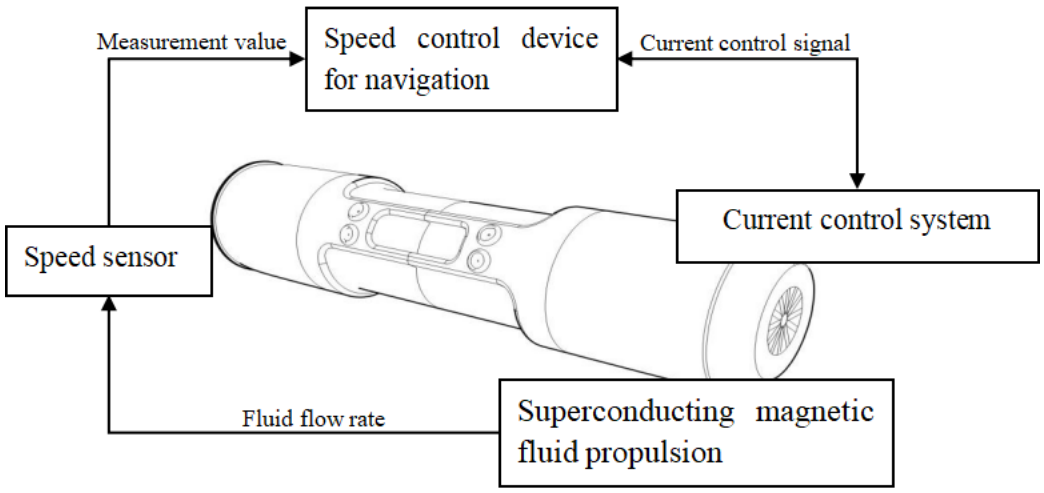

Figure. 3. Superconducting magnetic fluid propulsion device.

In order to ensure the stable and efficient operation of underwater vehicles in waters with different densities, we have designed an environmental intelligent electrolyte management system. This system integrates two core components: an intelligent electrolyte adder and a closed-loop electrolyte recovery mechanism. The adder located at the inlet of the fluid channel accurately measures the added electrolyte according to the real-time detected water salinity information, which effectively enhances the conductivity of the fluid in fresh water or low-salinity seawater, and overcomes the problem of efficiency attenuation of traditional magnetic fluid propulsion in atypical waters. At the same time, the electrolyte recovery device located at the outlet of the channel is equipped with different ion exchange membranes, so that the salinity inside and outside the device can maintain a certain difference [14], and at the same time, the electrolyte can be obtained directly from the seawater to realize the recycling of electrolyte resources. It not only prevents the ecological interference of natural waters during the operation, but also reduces the navigation marks, which greatly enhances the concealment and environmental friendliness of the vehicle. The device ensures that underwater exploration and mission execution of underwater robots are more flexible, efficient, safe and environmentally friendly.

2.2 Sacrificial anode inspection devices

Aiming at the high cost of underwater oil and gas pipeline detection and the high risk of diver operations in underwater, this design proposes a sacrificial anode inspection device specifically designed to slow down the surface corrosion of underwater oil and gas pipelines. This device combines bionics and precision detection technology, supplemented by intelligent navigation, aiming to enhance the efficiency and safety of the robot in underwater detection work, while reducing the cost of oil and gas pipeline maintenance.

The core detection part of the sacrificial anode inspection device is located in the bottom of the robot, which is protected by the crab shell dome of the robot head to avoid the damage

and influence of the underwater high-pressure environment on the precision technical equipment. Sacrificial anode inspection device external shape is shown in Figure 4. The monitoring device integrates the magnetic probe and potential measurement technology, which can directly measure the current output and potential of the sacrificial anode, and realize the instant protection and accurate monitoring of the cathode. This real-time analysis capability is crucial for predicting anode lifespan and performing preventive maintenance on oil and gas pipelines, effectively maintaining pipeline integrity and extending service life [15]. This real-time analysis capability is crucial for predicting anode life and preventive maintenance of oil and gas pipelines, which can effectively maintain pipeline integrity and prolong service life.

Figure. 4. Sacrificial anode inspection device.

In addition, the device uses GPS and high-precision map path planning [16] to pre-adjust the equipment, and then uses the visual system shown in Figure 2 to preliminarily scan the pipeline to identify the pipeline status and locate the anode. Anti-displacement crab legs closely adhere to the pipeline for precise maintenance, while magnetic probes and potential measurement electrodes work together to obtain key data reflecting anode performance [17]. These data are transmitted to the robot control center in real time for analysis. The control center system quickly evaluates the anode condition through the algorithm, and relies on the autonomous navigation and vision system to ensure the safety of the robot throughout the detection. Finally, the system automatically generates a detailed report on the pipeline and anode status, providing immediate feedback to the ground team to expedite maintenance decisions.

In the face of complex and changeable underwater environment, the sacrificial anode inspection device is equipped with an autonomous navigation and obstacle avoidance system to ensure that the underwater robot can still operate safely and continuously in unfavorable environments such as low visibility and strong water flow. And avoid the risk of staff diving operations, while ensuring that the detection task is fully and efficiently completed. The device not only overcomes the problems of traditional underwater pipeline detection, but also lays a solid technical foundation for ensuring the safe operation of underwater oil and gas pipelines and improving maintenance efficiency. Although the initial investment of the device is high, it can achieve rapid cost recovery in the short term and long-term stable profit

by reducing the cost of manual detection, improving the detection efficiency and reducing the number of pipeline maintenance or replacement.

2.3 Anti-displacement crab legs

Aiming at the anti-displacement crab leg device, which is the core part of the underwater robot motion designed in this paper, we take the robot 's smooth underwater movement as the condition and one of the crab legs as the research target. As shown in Figure 5, we establish a two-dimensional plane kinematics model [18]. Joint AB is coupled with adjacent manipulators and anti-displacement legs, and the rotation angle can be adaptively adjusted by the command sent by the control system to establish the attitude. The joint AB is the mechanical arm, which is responsible for controlling the rotation of the whole leg in the plane. The joint BC is the anti-displacement leg part, and its leg tip is sharp and hard. It can carry out detailed landing control after the main direction of the arm is determined. It can easily move on soft or rugged seabed terrain, maintain stability during sampling operations and grip control at the landing position, and drive the whole robot to move.

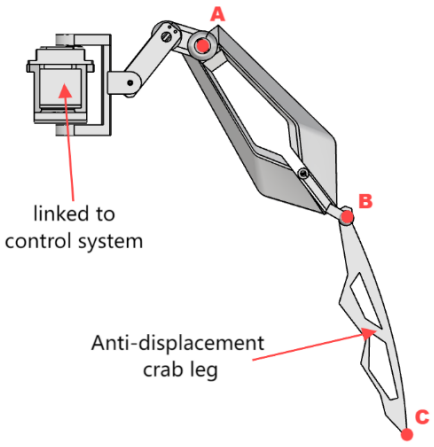

Figure. 5. The detail of Anti-displacement crab leg

Comparing the state of the joint movement in Figure 6, the angle change of joint OA drives the mechanical arm AB to extend forward, and the anti-displacement crab leg BC is perpendicular to the ground in a fixed attitude. The illustration shows that the forward movement posture of the crab-like underwater robot changes continuously and the movement changes smoothly, which will not lead to too much mechanical vibration and is conducive to the smooth movement of the robot during underwater operation. The reasonable division of labor between the mechanical arm and the leg ensures that the movement of the robot is less hindered when working underwater. The six anti-displacement crab legs are reasonably distributed, and the free regulation in three-dimensional space [19]is realized through the spherical link module [20], which greatly enhances the flexibility of the robot motion and improves the mechanical life of the robot. The robot's stability during underwater operations is further improved by alternating between two postures to achieve movement on a plane.

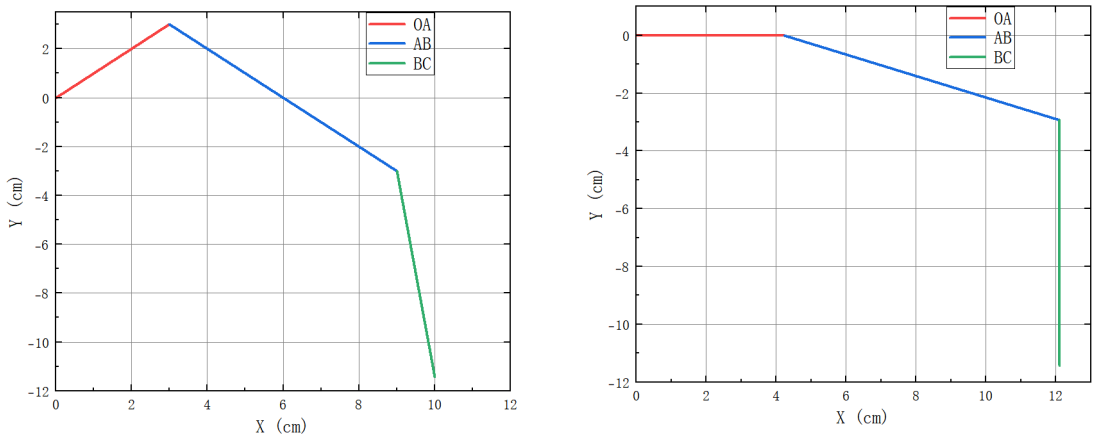

Figure. 6. Anti-displacement crab leg joint. The left one is the initial posture. The right one is the forward movement posture.

As shown in Figure 7, using the Monte Carlo method [21], a set of mapping points for the workspace of the anti-displacement crab legs' fingertip was obtained. The space between the fingertip and the end of the manipulator represents the activity range of the anti-displacement crab legs. Once the joint lengths are determined, the workspace area of the legs can be established. Joint space trajectory planning is used to ensure smooth leg trajectories and to avoid shocks during the movement of the anti-displacement crab legs. Ample space is reserved for the manipulator to perform maintenance or sampling tasks.

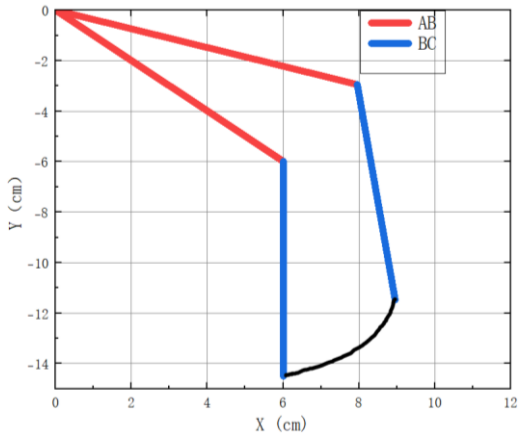

Figure. 7. The approximate activity range of the anti-displacement crab leg.

3. Computational process

3.1 Attitude control

When a robot performs tasks underwater, maintaining the correct attitude is crucial as it directly affects its operational efficiency, safety, and task completion. Using a PID control algorithm to manage the robot's attitude is a common and effective method [22]. The PID control algorithm not only responds quickly to attitude changes but also eliminates steady-state errors through integral action and uses differential prediction to avoid excessive

adjustments, ensuring that the robot can perform tasks precisely and efficiently while maintaining the correct attitude in the complex and dynamic underwater environment. The control principles are as follows:

$$u(t)=K_{\mathrm{p}}\left[e(t)+\frac{1}{T_{\mathrm{I}}}\int_0^t e(t)\mathrm{d}t+T_{\mathrm{D}}\frac{\mathrm{d}e(t)}{\mathrm{d}t}\right] \tag{1}$$

K_{p} is the proportional gain coefficient, T_{I} is the integral time constant, T_{D} is the derivative time constant. $u(t)$ is the output value of the PID control system, used to drive actuators, such as inverters or regulating triggers, to achieve precise control. $e(t)$ is the error signal of the PID system, representing the difference between the desired value and the actual measured value.

3.2 Force analysis

When the robot is inspecting the pipeline, it experiences thrust from two superconducting magnetic fluid F_{e} propulsion devices, water resistance $\mathrm{F_{f1}}$, and frictional force F_{f2} between the clamping mechanism and the pipeline, the support force F_{k} provided by the clamping mechanism. This can be expressed as:

$$\sum F_{\mathrm{x}}=2F_{\mathrm{e}}-F_{\mathrm{f1}}-F_{\mathrm{f2}}=0 \tag{2}$$

$$\sum F_{\mathrm{y}}=N-G-F_{\mathrm{k}}=0 \tag{3}$$

The formula for calculating the fluid resistance of water F_{f1} acting on the robot underwater is [23]:

$$F_{\mathrm{f1}}=C_{\mathrm{d}}Av^2\rho \tag{4}$$

In the formula, A is the projected area of the robot in the direction of motion; v^2 is the square of the robot's velocity; C_{d} is the empirical fluid resistance coefficient and ρ is the density of the fluid in the underwater environment.

The thrust of the underwater robot's propulsion system comes from the superconducting magnetic fluid propulsion device. In the area affected by the device, the electromagnetic force F_{e} on the seawater is:

$$F_{\mathrm{e}}=\int_{V_{\mathrm{d}}} JB\sin\theta_{\mathrm{e}}\mathrm{d}V \tag{5}$$

In the formula, V_{d} is the effective volume of the superconducting magnetic fluid device's channel; J is the current density; B is the magnetic flux density; and θ_{e} is the angle between the current and the magnetic flux. When the current density and magnetic flux density are uniformly and stably distributed and perpendicular to each other, the formula can be simplified to:

$$F_{\mathrm{e}}=JBV_{\mathrm{d}} \tag{6}$$

3.3 Degrees of freedom calculation

The number of degrees of freedom represents the number of actuators required for the robot mechanism to achieve specific motion. The calculation of the mechanism's degrees of freedom is the total number of degrees generated by the moving parts minus the total number of constraints caused by higher pairs P_{H} and lower pairs P_{L} [24]. The formula is:

$$F=3n-(2P_L+P_H) \tag{7}$$

3.4 Mechanical working pressure

The underwater robot relies on a superconducting magnetic fluid propulsion device as its main power source [25]. Under ideal conditions, the working pressure P of the superconducting magnetic fluid propulsion device is equal to the electromagnetic force F_e per unit area [26]. The formula is:

$$P=\frac{F_e}{S_d}=JBL \tag{8}$$

In the formula, S_d is the effective force area of the superconducting magnetic fluid device, and L is the effective magnetic field working length of the superconducting magnetic fluid device drive system.

4. Conclusion

Inspired by the natural movement of crabs in underwater environments, and addressing issues such as the variability of underwater environments, complex geological conditions causing difficulties in underwater movement, and the susceptibility of underwater robots to damage, a crab-like underwater robot has been designed. This robot utilizes superconducting magnetic fluid propulsion device and sacrificial anode inspection device to reduce underwater operational costs and enhance sampling efficiency. It also features anti-displacement crab legs to improve the robot's operational range underwater.

The superconducting magnetic fluid propulsion system serves as the main power source for the robot. It uses seawater as the conductive fluid and generates thrust through the interaction of electromagnetic fields, directly propelling the fluid. By integrating gas-liquid two-phase flow technology with the superconducting magnetic fluid propulsion, the robot efficiently converts the kinetic energy of gas into water flow kinetic energy. This overcomes the cavitation hazards associated with traditional propellers and addresses the low efficiency of conventional magnetohydrodynamic propulsion underwater.

The robot's lower abdomen is equipped with a sacrificial anode inspection device integrated with magnetic probe head and potential measurement technology. This device provides real-time monitoring and protection of underwater oil and gas pipelines, ensuring their safe operation and improving maintenance efficiency while reducing labor costs.

Finally, the movement of the anti-displacement crab leg on the flat ground is analyzed on the two-dimensional plane, and the working space and joint trajectory of the anti-displacement crab leg on the flat water bottom are simulated. Combined with the PID attitude control algorithm, the degree of freedom calculation shows that the pose and motion process of the anti-displacement crab leg are in line with the scientific design, and the motion state is stable. In addition, the working pressure analysis and force analysis of the robot are also carried out. Figure 8 shows the robot performing maintenance on oil and gas pipelines in an actual underwater environment. These analyses show the excellent impact resistance and flexible maneuverability of the underwater robot. The above design analysis shows that this kind of crab-like underwater control system has good engineering reference value.

Figure. 8. Imagined actual work scene of the underwater robot.

References:

1. Haiming Wang, Characteristics and prospects of global offshore oil and gas exploration and development. Chemical Engineering and Equipment. 2022; 12: 212-213+167.
2. Junhao Zhang, *et al.* Modeling and control simulation of a bio-inspired underwater snake robot with a novel rigid–soft coupling structure. Chinese Journal of Engineer ing. 2023; 45(12): 2095-2107.
3. Xuehai Zhang, *et al*. Modeling and simulation of cuttlefish-imitating underwater sampling manipulators. Journal of Mechanical and Electrical Engineering. 2024; 48(6): 58-64.
4. Dongdong Zhang, *et al*. Structural design and experimental study of underwater robots based on biomimetic jellyfish. Mechanical & Electrical Engineering Maga zine. 2024; 41(4): 739-746.
5. Larabi-Marie-Sainte Souad, *et al*. Locomotion of bioinspired underwater snake ro bots using metaheuristic algorithm. Computers, Materials & Continua. 2022; 72 (1): 1293-1308.
6. Torres Eliseo de J. Cortés, *et al*. Mechanical design of a new hybrid 3R-DoF b ioinspired robotic fin based on kinematics modeling and analysis. Actuators. 202 4; 13(9): 353-353.
7. Loskutova Tetiana, *et al*. Corrosion resistance of coatings based on chromium a nd aluminum of titanium alloy Ti-6Al-4V. Materials (Basel, Switzerland). 2024; 17(15): 3880-3880.
8. Sharma R. K., *et al*. Effect of varying chromium and titanium content on corro sion, mechanical and solid particle erosion properties of iron alloy based coating. Materialwissenschaft und Werkstofftechnik. 2022; 53(6): 675-685.
9. Luchkina L. V., *et al*. Study of physical and mechanical properties of laboratory and industrial samples of heat insulating materials used for the production of p

re-insulated pipes, fi ttings and polyurethane shells. Plasticheskie Massy. 2022; 1 (11-12): 50-55.
10. Saite Wu, Prospects for the application of magnetohydrodynamic propulsion tech nology in marine vessels. Mechanical and Electrical Information. 2020; 36: 74-7 5.
11. Youguang Ma, *et al*. Progress of studies on gas-liquid two-phase flow in microc hannels. Chemical Industry and Engineering Progress. 2007; 8: 1068-1074.
12. Yibo Feng, et al. Study on the transition boundary between bubbly flow and slu g flow in gas-water two-phase descending flow. Special Oil and Gas Reservoirs. 2024; 31(2): 166-174.
13. Fukasawa Satoshi, *et al*. Effect of small rectangular channel height on bubble m oving velocity in gas-liquid two-phase flow through sudden contraction. Japanese Journal of Multiphase Flow. 2013; 27(2): 168-174.
14. Qianqian Ge, *et al*. Perspective in ion exchange membranes. Chemical Industry and Engineering Progress. 2016; 35(6): 1774-1785.
15. Shixin Hu. Present status and prospect of cathodic protection for pipeline. Corro sion and Protection. 2004; 3: 93-101.
16. Guo Xuan, *et al*. Autonomous underwater vehicle path planning based on impro ved salp swarm algorithm. Journal of Marine Science and Engineering, 2024; 12 (8): 1446-1446.
17. Kankan Qi, *et al*. Test and analysis of fluxgate sensor probe. Electronic Test. 2 020; 1: 41-44.
18. Junwei Shen, *et al*. Trajectory planning optimization of two-degree-of-freedom p arallel mechanism. Journal of Mechanical Transmission. 2021; 45(7): 110-115.
19. Derya Kahveci, *et al*. Geometric kinematics of persistent rigid motions in three-dimensional minkowski space. Mechanism and Machine Theory. 2022; 167.
20. Alwan Hassan Mohammad, *et al*. Motion control of three links robot manipulato r (open chain) with spherical wrist. Al-Khawarizmi Engineering Journal. 2019; 1 5(2): 13-23.
21. Baofeng Li, *et al*. Calculation of space robot workspace by using monte carlo method. Spacecraft Engineering. 2011; 20(4): 79-85.
22. Wenliang Zhu, *et al*. Design of PID control system for underwater robots. Marit ime Safety. 2024; 6: 1-3.
23. Chuanhui Zhou, *et al*. Calculational methods about the friction factor of fluid. R efrigeration and Air Conditioning. 2004; 3: 35-36.
24. Yuxian Zhang, *et al*. Exploration on the formula of degree of freedom of space mechanism. Journal of Chongqing University (Natural Science Edition). 2003; 9: 53-55.
25. Tiankui Wang, *et al*. Prospects in marine application of superconductive magneto -hydrodynamic thruster. Ship Engineering. 1994; 5: 9-13+8-2.
26. Zhen Yi, *et al*. Research on technology of ship magnet-hydrodynamic propulsio n. Marine Technology. 2002; 1: 3-5+12.